



UWL REPOSITORY

repository.uwl.ac.uk

A compact quint-band bandpass filter based on stub-loaded resonators

Farhat, Mohamad, Munisami, Jagadissen, Abdul-Niby, Mohammed and Nahas, Michel (2017) A compact quint-band bandpass filter based on stub-loaded resonators. Engineering, Technology & Applied Science Research, 7 (3). pp. 1694-1698. ISSN 2241-4487

This is the Published Version of the final output.

UWL repository link: <https://repository.uwl.ac.uk/id/eprint/3834/>

Alternative formats: If you require this document in an alternative format, please contact: open.research@uwl.ac.uk

Copyright: Creative Commons: Attribution 3.0

Copyright and moral rights for the publications made accessible in the public portal are retained by the authors and/or other copyright owners and it is a condition of accessing publications that users recognise and abide by the legal requirements associated with these rights.

Take down policy: If you believe that this document breaches copyright, please contact us at open.research@uwl.ac.uk providing details, and we will remove access to the work immediately and investigate your claim.

A Compact Quint-Band Bandpass Filter Based on Stub-Loaded Resonators

Mohamad Farhat

School of Engineering
The Australian College of
Kuwait, Kuwait
m.farhat@ack.edu.kw

Jagadissen Munisami

School of Computing and
Engineering
University of West London
United Kingdom
kevin.munisami@uwl.ac.uk

Mohammed Abdul-Niby

School of Engineering
The Australian College of
Kuwait, Kuwait
m.nibi@ack.edu.kw

Michel Nahas

School of Engineering
The Australian College of
Kuwait, Kuwait
m.nahas@ack.edu.kw

Abstract—This paper presents a planar quant-band bandpass filter with a high out-of-band rejection. The filter is based on inter-coupled stub-loaded resonators, where pairs of resonators are electromagnetically coupled to each other and the feed lines. This results in excitation of passbands, where the first and the third passbands are generated by $\lambda/4$ stub-loaded resonators. The second and the fifth passbands are excited by $\lambda/2$ stub-loaded resonators. And the fourth passband is generated by $\lambda/2$ resonators. The proposed technique provides sufficient degree of freedom to control the center frequency and bandwidth of the five passbands. In addition, the seven transmission zeros created around the passbands results in a quant-band filter with high selectivity, sharp 3dB cut-off frequency, high isolation, and low passband insertion-loss. Design methodology and simulation results of the filter are provided.

Keywords—Quant-band; stub-loaded resonators; microstrip filter; planer filter

I. INTRODUCTION

Nowadays, there is a high need for high performance miniature microwave bandpass filters having a low production cost, compact size, low insertion losses and high passband selectivity for the rapidly evolving wireless communications market, such as satellite and mobile communication systems. In addition there is a high demand for multiband bandpass filters in wireless communication devices such as RF transceivers to operate in multiple but separated frequency bands so that users can access various services, such as WLAN, IEEE 802.16 (WiMAX) and RFID, with a single multimode handset or terminal. Higher order bandpass filters are routinely modelled by cascading multiple single/dual-mode resonators. This straightforward approach results in an significant increase in the overall filter size and raises the fabrication cost. However, although many different methods [1-5] have been reported in generating multiband in a single configuration, the main problems still exist and it is due to difficulties in achieving good performance for all passbands, especially with more than three passbands. So far, most reported work with multiple band are limited to four or less [1-4] and only few methods have been reported on Quint-band bandpass or more filters [5-7].

In [1], a multi-band filter using CPW-fed dual-mode double-square ring resonators was proposed. The resonant frequencies were controlled by tuning the perimeter ratio of the square rings. The bandwidth of the four passbands is different with high insertion loss. Another design [2] implemented a multi-band filter by loading a transmission-line with either open or short-circuited stubs in a parallel configuration. This technique requires an optimization method to control both the center frequency and the bandwidth of the filter. However, this technique occupies a high area with a dimension of $1.09\lambda_g \times 0.76\lambda_g$. The multi-band filter in [3] is based on inserting two stepped-impedance resonators (SIR). The filter's passbands can be individually controlled by modifying the dimensions of the SIRs. Although the resulting filter is miniature in size, the 3dB roll-off is skirt not sharp. In [4] a pair of square-ring loaded resonators is used to excite quadruple-modes. The two resonators are connected to each other with a microstrip-line and are coupled to the input and output feedlines. This filter was fabricated on a 2-inch diameter 0.5mm thick MgO wafer of dielectric constant 9.8 with double-sided YBa₂Cu₃O_y thin films. The size of the filter is $0.37\lambda_g \times 0.45\lambda_g$. However this filter is very expensive as it needs to be cooled to a temperature of 77K. In [5], a quint-band BPF using tri-mode stub-loaded SIRs was proposed. This filter cascaded five sets of tri-mode resonators along feeding lines. Despite being a simple design, the insertion losses are around 3dB and occupied a wide area. A compact double-layered quint-band BPF comprising three pairs of microstrip SIRs and two pairs of slot resonators was reported in [6]. This type of filter is not only difficult to manufacture but also exhibits unacceptable insertion-loss resulting from multilayer properties. In [7] a quint-band BPF combining multimode resonator and $\lambda/4$ resonators was reported. However, this design occupies the relatively low 3dB fractional bandwidths (FBWs).

In this paper, a novel Quint-band bandpass filter structure is proposed and is based on inter-coupled $\lambda/4$, $\lambda/2$ stub-loaded and $\lambda/2$ resonators. The first and third passbands are determined by the $\lambda/4$ stub-loaded resonator, and the second, fifth passbands by the $\lambda/2$ stub-loaded resonator the fourth passband by the $\lambda/2$

resonator. The proposed Quint-band filter generates seven transmission zeros located around the passbands to realize high selectivity, sharp 3dB roll-off and high out-of-band rejection. The planar structure facilitates the design and reduces fabrication cost. With a size of $0.35\lambda_g \times 0.3\lambda_g$, the filter is miniature compared to the aforementioned filters and this eases integration in wireless systems. The filter structure provides sufficient degree of freedom to control the center frequency and bandwidth of the five passband responses. The filter was designed and simulated at 2.4/3.5/4.9/5.8/6.7 GHz for different applications such as WLAN and WiMAX amongst others.

II. FILTER CONFIGURATION AND ANALYSIS

A. Resonators Configuration

Figure 1 shows the configuration of the proposed filter. It consists of six resonators. Stub-loaded resonators 1 and 2 are $\lambda/2$ open-circuited at the coupling ends, and their other ends are parallel coupled to the $50\ \Omega$ input/output feedlines of width W_1 as shown in Figure 2(a). Resonators 3 and 4 are $\lambda/2$ resonators embedded inside resonators 1 and 2 for size reduction as shown in Figure 2(b). The stub-loaded resonators 5 and 6 are $\lambda/4$ short-circuited at the coupling ends, and are also parallel coupled with the feedlines as shown in Figure 2(c). The $\lambda/4$ stub-loaded resonators (1 and 2) excite the first and third passbands in the filter response, resonators 3 and 4 excite the fourth passband and the $\lambda/2$ resonators (3 and 4) excite the second and fourth passbands.

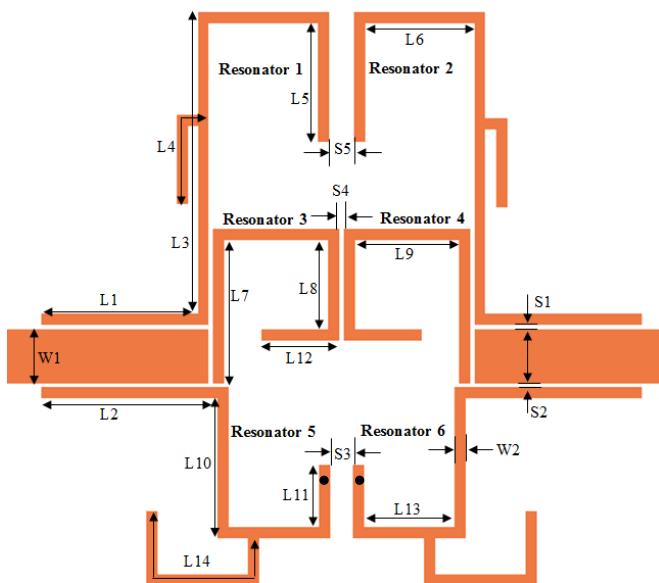


Fig. 1. Layout of the proposed quad-band bandpass filter structure.

B. Analysis of the Quint-Band Bandpass Filter

The structure of the proposed $\lambda/2$ and $\lambda/4$ stub-loaded resonators are shown in Figure 3(a) and Figure 4(a), respectively. In Figure 3(a), the $\lambda/2$ microstrip resonator is defined by parameters L_A , L_B , Z_1 and Z_2 that denote the length and characteristic impedance of the microstrip-line and open-stub, respectively. Odd and even-mode analysis can be used to characterize the resonator. Figure 3(b) and 3(c) show the odd

and even-mode equivalent circuits, respectively. The odd and even frequencies are given by [8]:

$$f_{odd} = f_2 = \frac{nc}{2L_A \sqrt{\epsilon_{eff}}} \quad (1)$$

$$f_{even} = f_5 = \frac{nc}{(L_A + 2L_B) \sqrt{\epsilon_{eff}}} \quad (2)$$

Where ϵ_{eff} is the effective dielectric constant, n is the mode number ($n = 1, 3, 5, \dots$) and c is the speed of light in free space (3×10^8 m/s).

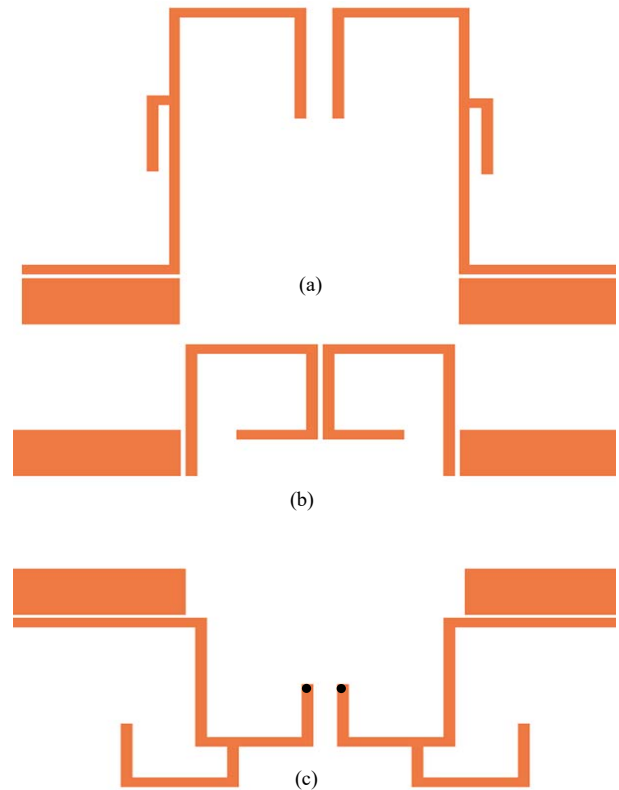


Fig. 2. Structure of the proposed filter, (a) $\lambda/2$ stub-loaded resonator, (b) $\lambda/2$ resonators, and (c) $\lambda/4$ stub-loaded resonator.

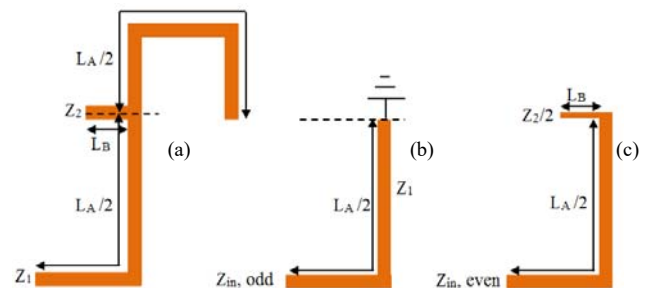


Fig. 3. (a) Structure of the proposed $\lambda/2$ stub-loaded resonator, (b) odd-mode equivalent circuit, and (c) even-mode equivalent circuit.

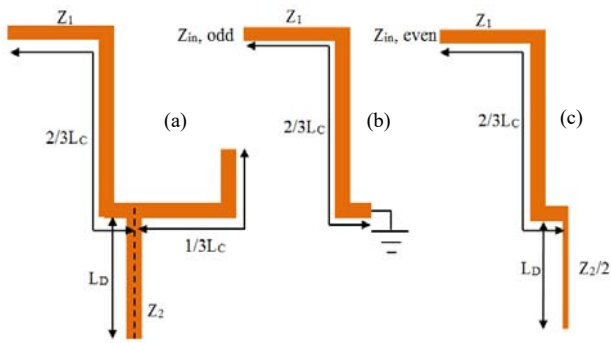


Fig. 4. (a) Structure of the proposed $\lambda/4$ stub-loaded resonator, (b) odd-mode equivalent circuit, and (c) even-mode equivalent circuit.

The $\lambda/4$ stub-loaded resonator in Figure 4(a) is defined by L_C , L_D , Z_1 and Z_2 , denoting the length and the characteristic impedance of the microstrip-line and open-stub, respectively. Figure 4(b) and 4(c) show the odd and even-mode equivalent circuits, respectively, of the $\lambda/4$ stub-loaded resonator. The odd and even frequencies are given by:

$$f_{odd} = f_2 = \frac{nc}{2L_A \sqrt{\epsilon_{eff}}} \quad (3)$$

$$f_{even} = f_3 = \frac{nc}{(2L_C + L_B) \sqrt{\epsilon_{eff}}} \quad (4)$$

On the other hand, resonators 3 and 4 are $\lambda/4$ resonators which excite the fourth passband, and its centre frequency is given by:

$$f_4 = \frac{nc}{2L_E \sqrt{\epsilon_{eff}}} \quad (5)$$

where $L_E = L_7 + L_8 + L_9 + L_{12}$

C. Feed and Coupling Scheme

Figure 5 shows the feed and coupling schemes employed in the filter, where the black and hollow circular nodes represent resonators and source/load respectively. Figure 5(a) represents the feed and coupling scheme at the first (f_1) and the third (f_3) resonant frequencies. The corresponding insertion-loss responses are shown in Figure 6. In contrast, the resonators 3, 4, 5 and 6 are non-resonating at f_1 and f_3 , but are however excited at other passbands. Similarly, Figure 5(b) shows the feed and coupling scheme at the fourth (f_4) resonant frequency. Figure 6 illustrates that resonators 1, 2, 5 and 6 are non-resonating at f_4 . Figure 5 (c) represents the feed and coupling scheme at the first (f_2) and the fifth (f_5) resonant frequencies. The corresponding insertion-loss response is shown in Figure 6. In contrast, the resonators 1, 2, 3 and 4 are non-resonating at f_2 and f_5 , but are excited at other passbands. Source to load coupling is inherently realized as the non-resonating nodes are directly coupled with the resonating nodes. The passband bandwidth of the filter depends on the external Q-factor and the coupling coefficient between the resonator pairs. In particular, this depends on the

gaps (S3, S4, and S5), the width (W2) and the lengths (L5, L8 and L11). Strong EM coupling between the resonators is shown by the intensity of the current in Figure 7. It is clear that only the desired resonator resonates at its associated frequency and form strong EM coupling.

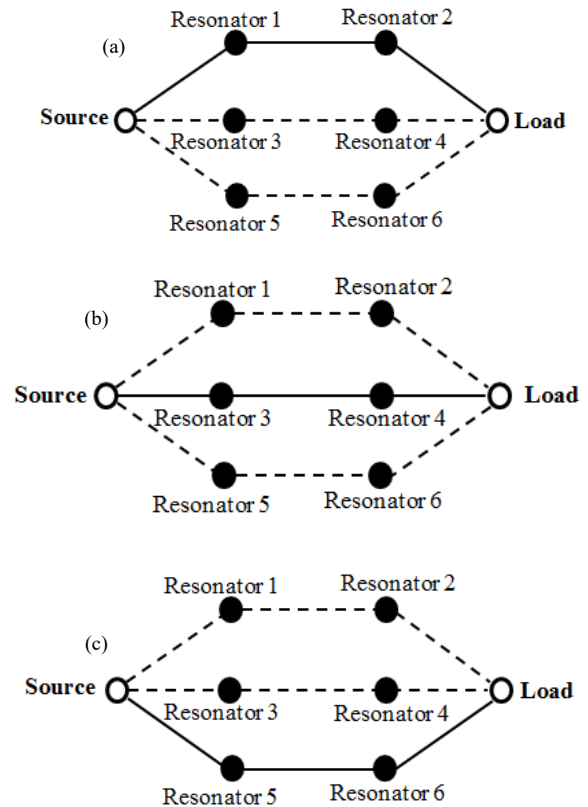


Fig. 5. Feed and coupling scheme, (a) at the first and third resonant frequencies, (b) at the fourth resonant frequency, and (c) at the second and fifth resonant frequencies

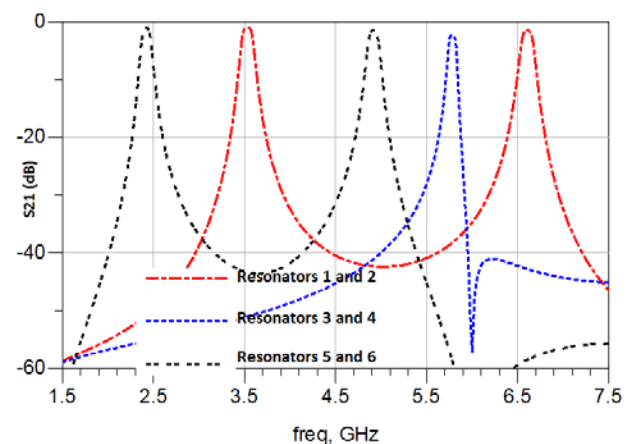


Fig. 6. Frequency response of the quad-band bandpass filter.

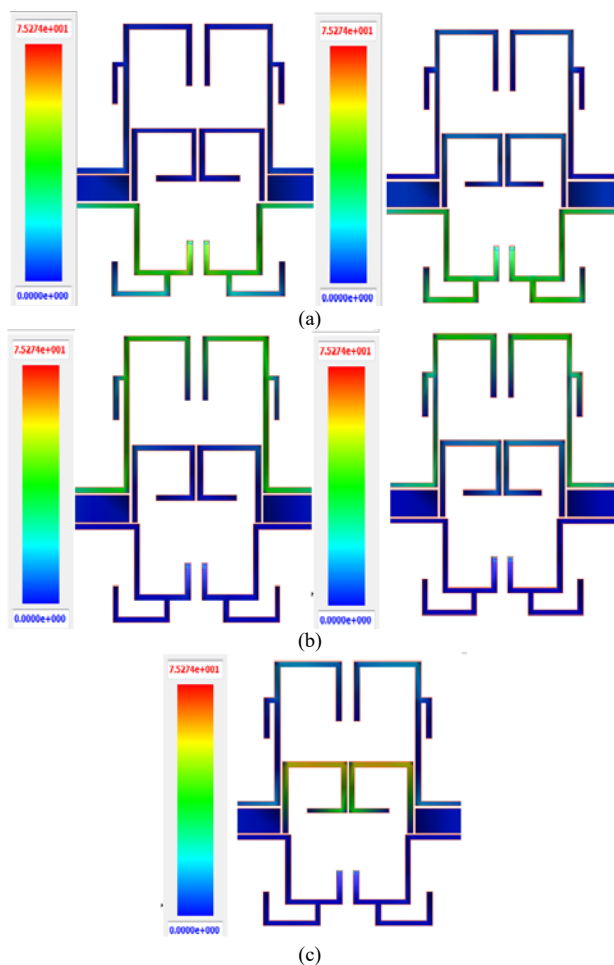


Fig. 7. The surface current distribution of the proposed filter (a) at the first (3 GHz), (b) the second (6.9 GHz) and (c) the third resonance frequency (8.6 GHz), respectively.

III. FILTER IMPLEMENTATION

The initial dimensions of the filter are determined based on the design specifications, in particular the desired passbands frequencies. Fine-tuning is then necessary to achieve the desired response using an appropriate simulation tool. Resonator pairs 5 and 6 determine the center frequency of the first and the third passbands and the lengths of the resonators can be calculated from (3) and (4). The length of the stub does not affect the fundamental resonant frequency f_1 but it can be used to control the frequency of the second harmonic of the resonator at f_3 . This means that the length L_C can be determined from f_1 and then the length of the open-stub (L_D) is fine tuned to obtain the desired f_3 . In this design technique the resonators have no loading effect over each other. Thus, the $\lambda/4$ stub-loaded resonators have no affect on f_2 and f_5 , as is evident from Figure 6. On the other hand, resonators 1 and 2 determine f_2 and f_5 according to (1) and (2). Similarly the length of the stub does not affect the fundamental resonant frequency f_2 but it can be used to control the frequency of the second harmonic f_5 . Therefore, f_2 can be determined by the length L_A , and the desired f_5 obtained through fine-tuning of the open-stub (L_B).

The resonant frequency f_4 is determined, characterized and controlled by resonators 3 and 4 according to (5).

The second step is to determine the required bandwidth for each passband. As previously stated, the bandwidth of the filter's passbands depends on the external Q-factor and the coupling-coefficient between resonators. However, in this design the three pairs of resonators have no coupling effect over each other. Thus, the bandwidth of the five passbands can be determined separately. The coupling-coefficient between the first and third passband depends on S3, W2 and L11, whereas the coupling-coefficient between the second and the fifth passbands depend on S5, W2 and L5, and the coupling-coefficient for the fourth passband depends on S4, W2 and L8. The external Q-factor is determined by L2, W2 and S2 for the first and third passbands, L1, W2 and S1 for the second and the fifth passbands, and W1, W2, and L7 for the fourth passband.

IV. SIMULATION RESULTS

To demonstrate the feasibility of the proposed concept, a quint-band filter was designed for fundamental resonant frequencies at 2.4/3.5/4.9/5.8/6.7 GHz. The filter was simulated on a substrate with a thickness of 0.76mm and relative dielectric constant of 2.17. Following the design methodology in the preceding section, the filter's dimensions were calculated to be (in millimeters): $L_1 = 5$, $L_2 = 5$, $L_3 = 13$, $L_4 = 4.5$, $L_5 = 5.8$, $L_6 = 4.9$, $L_7 = 6.24$, $L_8 = 5$, $L_9 = 4.65$, $L_{10} = 6.3$, $L_{11} = 2.8$, $L_{12} = 3.5$, $L_{13} = 4$, $L_{14} = 8$, $W_1 = 0.5$, $S_1 = 0.2$, $S_2 = 0.2$, $S_3 = 0.9$, $S_4 = 0.2$, $S_5 = 1.09$, and $W_2 = 2.42$, which corresponds to a characteristic impedance of 50Ω . Simulations were performed using Keysight Technologies' Momentum 3D planar EM simulator based on the method-of-moment (MoM). Figures 8-10 show the simulation results of the insertion-loss, return-loss and insertion/return losses respectively. The filter has five passband responses centered at 2.4/3.5/4.9/5.8/6.7 GHz with a high out-of-band rejection. The insertion-losses at the five passbands are less than 1dB, 1dB, 1.5dB, 1.3dB and 2dB, respectively. The corresponding return-losses are greater than 18dB, 17dB, 18dB, 20dB and 14dB, respectively. The seven transmission zeros between the passbands result in the realization of a filter with high selectivity and high isolation between adjacent passbands.

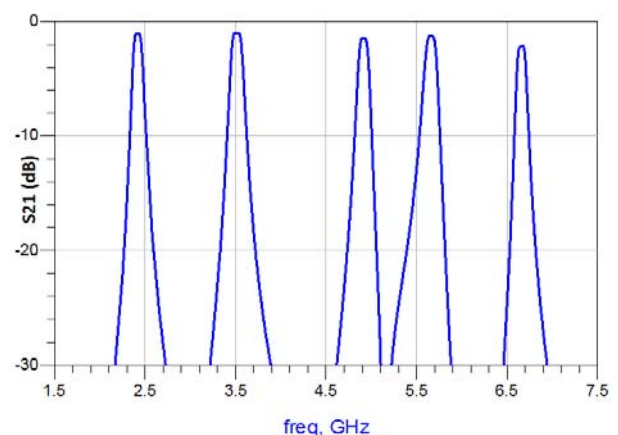


Fig. 8. Simulated insertion-loss response of the proposed filter.

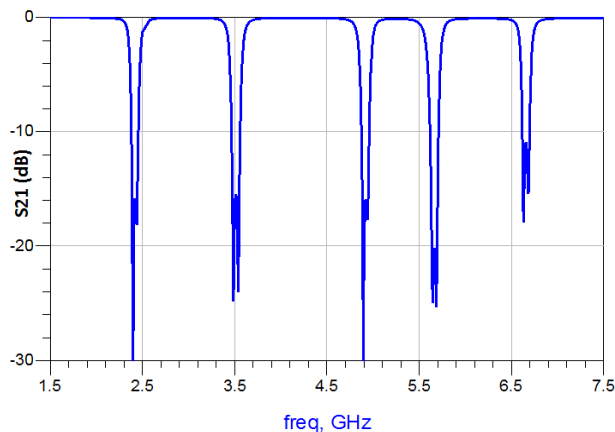


Fig. 9. Simulated return-loss response of the proposed filter.

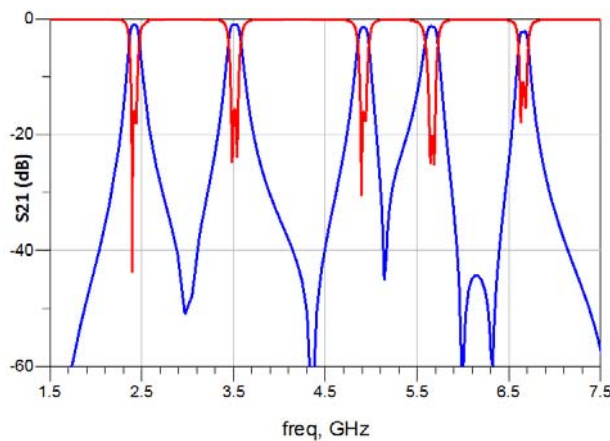


Fig. 10. Simulated insertion-loss and return-loss response of the proposed filter.

V. CONCLUSION

A highly compact planar quant-band bandpass filter based on stub-loaded resonators is presented. Three pairs of resonators are used to excite quant-mode resonances. The proposed technique provides a sufficient degree of freedom to alter the filter's specifications in terms of centre frequency and bandwidth. Source to load coupling and the resulting two transmission paths are inherently realized to create transmission zeros, resulting in high selectivity and high isolation between the five passbands. The design methodology has been verified through simulation results. The filter's performance and compact size makes it attractive for application in multiband wireless communication systems.

REFERENCES

- [1] J. C. Liu, J. W. Wang, B. H. Zeng, D. C. Chang, "CPW-fed dual mode double-square-ring resonators for quad-band filters", *IEEE Microw. Wireless Compon. Lett.*, Vol. 20, No. 3, pp. 142–144, 2010
- [2] C. Cui, Y. Liu, "Quad-band bandpass filter design by embedding dual-band bandpass filter with dual-mode notch elements", *Electronics Letters*, Vol. 50, No. 23, pp. 1719–1720, 2014
- [3] J. Xiao, Y. Zhu, Y. Li, X. Li, "Miniature quad-band bandpass filter with passband individually controllable using folded SIR", *Electronics Letters*, Vol. 50, No. 9, pp. 679–680, 2014
- [4] H. Liu, B. Ren, X. Guan, P. Wen, Y. Wang, "Quad-Band High-Temperature Superconducting Bandpass Filter Using Quadruple-Mode Square Ring Loaded Resonator", *IEEE Trans. on Microwave Theory and Techniques*, Vol. 62, No. 12, pp. 2931–2941, 2014
- [5] C. Chen, "Design of a compact microstrip quint-band filter based on the tri-mode stub-loaded stepped-impedance resonators", *IEEE Microw. Wireless Compon. Lett.*, Vol. 22, No. 7, pp. 357–359, 2012
- [6] K. Hsu, W. Hung, W. Tu, "Compact quint-band microstrip bandpass filter using double-layered substrate", *Proc. IEEE MTT-S, Int. Dig.*, Seattle, WA, USA, pp. 1–4, 2013
- [7] J. Ai, Y. Zhang, K. D. Xu, D. Li, Y. Fan, "Miniaturized quint-band bandpass filter based on multi-mode resonator and $\lambda/4$ resonators with mixed electric and magnetic coupling", *Microw. Wirel. Compon. Lett.*, Vol. 26, No. 5, pp. 343–345, 2016
- [8] X. Y. Zhang, Q. Xue, "Dual-band bandpass filter using stub-loaded resonators", *IEEE Microw. Wireless. Compon. Lett.*, Vol. 17, No. 8, pp. 583–585, 2007